第 48 回岩盤力学に関するシンポジウム講演集
公益社団法人土木学会　2022 年 1 月　講演番号 79

Investigation of applicability of DInSAR for monitoring ground surface displacements due to tunnel excavations - a case study in Korea

Wooseok KIM [1], Putu Edi YASTIKA[2] and Norikazu SHIMIZU[3]

[1] Senior Researcher, Korea Institute of Civil Engineering and Building Technology
(283, Goyang-daero, Ilsanseo-gu, Goyang-si, Gyeonggi-do, 10223, Rep. of Korea)
E-mail:kws@kict.re.kr
[2] Lecturer, Universitas Mahasaraswati Denpasar, Indonesia
(Jl. Soka No.47, Denpasar, 80237, Indonesia)
E-mail: ediyastika@unmas.ac.id
[3]Member of JSCE, Emeritus Professor, Yamaguchi University
(2-16-1 Tokiwadai, Ube 755-8618. Japan)
E-mail: nshimizu@yamaguchi-u.ac.jp

Key Words: *DInSAR, SBAS, ground surface displacement, monitoring, tunnel construction, urban area*

1. INTRODUCTION

Monitoring is important for assessing the stability of the ground and for confirming the validity of the design during the construction and operation of infrastructures. Monitoring is also useful for predicting risks, for managing safe operations, and for reducing project costs.

One of the important requirements of a monitoring system, employed during the construction and operation of infrastructures, is that it be able to monitor the behavior of the ground over extensive areas at a reasonable cost and with reasonable accuracy.

There are various types of instruments for field measurements in Geotechnical Engineering, such as extensometers, inclinometers, etc. Although they are useful, these instruments may not be adequate for monitoring large structures and extensive areas because they can only be applied to limited areas.

On the other hand, DInSAR (Differential Interferometric Synthetic Aperture Radar), using satellite-based radar, is capable of overcoming the above issues. This is because it can be applied to monitor the time-transition of the spatial distribution of ground surface displacements over extensive areas without the need for any devices on the ground[1)].

Many applications of DInSAR have already been studied for monitoring and detecting displacements. The second and third authors and their colleagues have applied DInSAR to monitor ground subsidence[2)-4)], landslides[5)-7)], a mining slope[8)], ground movements due to volcanic activity and an earthquake[9)-11)], and a dam embankment[12)].

The aim of this study is to investigate the applicability of DInSAR for monitoring the ground surface displacements above a tunnel construction site in Busan, Republic of Korea.

2. OUTLINE OF SAR AND DInSAR

SAR (Synthetic Aperture Radar) is a high-resolution radar device that is mounted on an artificial satellite. It operates day and night regardless the weather conditions. The SAR satellite travels on ascending (northward) and descending (southward) orbits (**Fig. 1**).

InSAR is a method for taking the signal phase difference from two scenes of SAR data, which are observed in the same area at different times. DInSAR is a technique for providing the displacement distribution of the Earth's surface based on the following equation[1]:

$$\Delta\varphi = \frac{4\pi}{\lambda} d_{LOS} + \Delta\varphi_{topo} + \Delta\varphi_{orb} + \Delta\varphi_{atmo} + \Delta\varphi_{scatt} + \Delta\varphi_{noise} \quad (1)$$

where $\Delta\varphi = \varphi - \varphi_{topo} - \varphi_{flat}$ can be computed by removing the contribution of the topography, φ_{topo}, and the phase effect due to the distance between two satellite positions, φ_{flat}, from the interferogram, φ (phase difference observed by SAR). d_{LOS} is the unknown ground surface displacement along the radar beam direction between a satellite and the Earth's surface; it is called the Line of Sight (LOS) displacement (**Fig. 2**). λ is the wavelength of the microwave transmitted from SAR. $\Delta\varphi_{topo}$ is the residual phase due to the error in the topographic elevation of the Earth's surface, $\Delta\varphi_{orb}$ is the residual phase due to the use of the inaccurate satellite orbital position, $\Delta\varphi_{atmo}$ is the effect of the atmospheric phase delay, $\Delta\varphi_{scatt}$ indicates the phase scatter due to changes in the conditions on the ground surface, and $\Delta\varphi_{noise}$ is the phase due to the noise contribution.

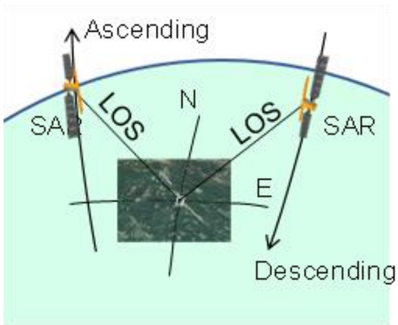

Fig. 1 Ascending and descending orbits of SAR satellite

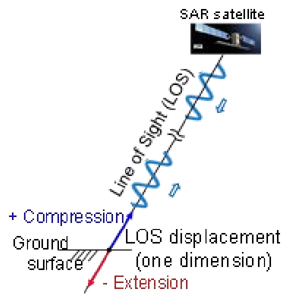

Fig. 2 Line of sight and LOS displacement

Small Baseline Subset (SBAS) DInSAR[13] is employed in this study to obtain the spatial distribution and temporal transition of the surface displacements. SBAS-DInSAR utilizes a series of SAR images in a target area and conducts multi-temporal DInSAR processing to produce the distribution of spatio-temporal LOS displacements.

3. STUDY AREA

An urban highway connecting Mandeok and Centum City in Busan, Republic of Korea, was approved as a construction project based on a private investment (**Fig. 3**). A total of 783.2 billion won, including a private investment of 588.5 billion won, will be used to construct the four-lane highway, each lane having a length of 9.62 kilometers[14].

This highway is expected to greatly reduce the commute between Mandeok and Centum City from the current 40 minutes to just 10 minutes. The construction was begun in 2019 and is expected to be finished in 2024. About 10% of the entire construction has been completed thus far (October 2021).

The area for applying SBAS-DInSAR in this study is shown in **Fig. 3**[15].

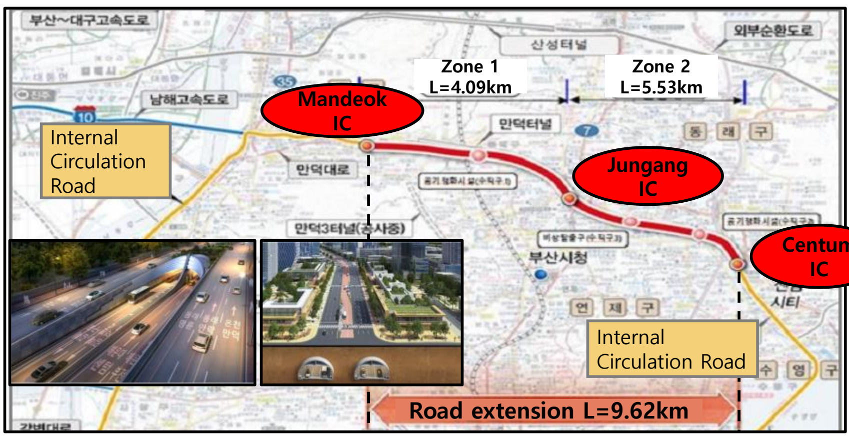

Fig. 3 Schematic plan view of tunnel construction site in Busan[15]

4. SAR DATASETS AND ANALYSIS

(1) Datasets

Sentinel 1A/B SAR data were used for the SBAS-DInSAR analysis. The analyzed SAR data comprise 165 images taken in the right-looking descending orbit with the Sentinel's path number 61. The period of data acquisition was from 25 May 2015 to 11 January 2021.

In the same period, 152 SAR data images were taken in the ascending orbit. However, there are blank (no data available) periods between 9 January 2018 and 14 June 2018, for a half year; and thus, the data are not continuous. Therefore, an SBAS-DInSAR analysis for the ascending data was conducted by dividing the datasets into two periods of 2 November 2014 to 9 January 2018 and 14 June 2018 to 21 August 2021.

Fig. 4 shows a footprint of the SAR data. The monitoring target area is marked by a yellow polygon. All Sentinel-1 A/B SAR data were provided by the European Space Agency at no charge.

To remove the topography component from the interferogram, a Digital Elevation Model (DEM) was used. The DEM data using ALOS World 3D (AW3D) DEM with a 30-meter spatial resolution was employed. This DEM was provided free of charge by the Japanese Aerospace Exploration Agency (JAXA).

(2) Data Processing – SBAS DInSAR

The SAR data were analyzed with the SBAS-DInSAR method[13] which is implemented in the Envi-SARscape 5.6 (Harris Geospatial Solutions, Inc.). On the one hand, 705 interferograms were analyzed using 165 ascending images. **Fig. 5** (a) shows the connection graph for the descending data, which represents the time-position table (the relative position/distance of the pair of satellites vs. the acquisition date of the data) of the SAR data used in the SBAS analysis. On the other hand, 163 and 314 interferograms were analyzed using 152 ascending images in the periods of 2014 to 2018 and 2018 to 2021, respectively (**Figs. 5** (b) and (c)).

Some interferograms were affected by the various error sources. In order to reduce the errors, processes called re-flattening and refinement were carried out. At the first stage of the analysis, 68 ground control points (GCPs) were selected and set over the observation area, assuming that the ground around the GCPs was stable. The coherence threshold values were set at 0.2 and 0.3 for the cases of using the descending and ascending data, respectively, and the spatial resolution of the ground was about 15 m by 15 m.

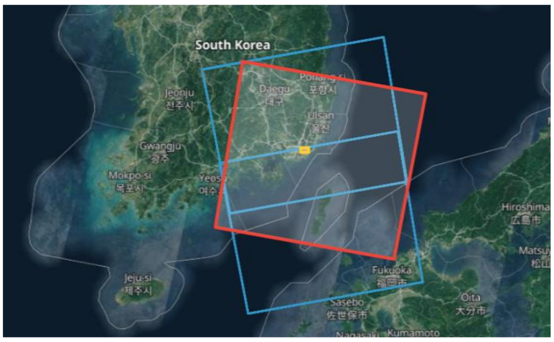

Fig. 4 Areas covered by Sentinel-1 data are in red (descending) and blue (ascending) boxes, while the study area is marked by a yellow box on the map.

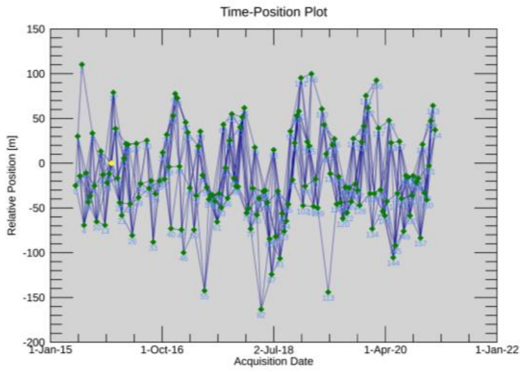

(a) Descending (25/5/2015-11/1/2021)

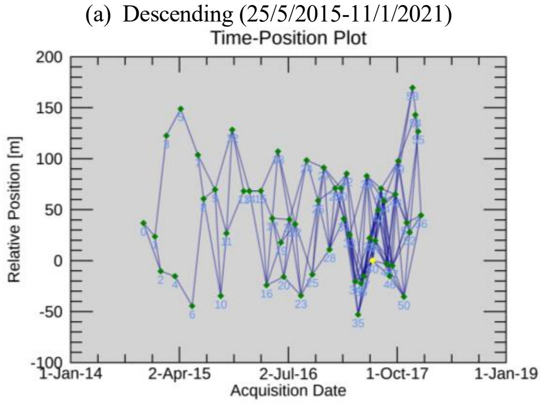

(b) Ascending (2/11/2014 - 9/1/2018)

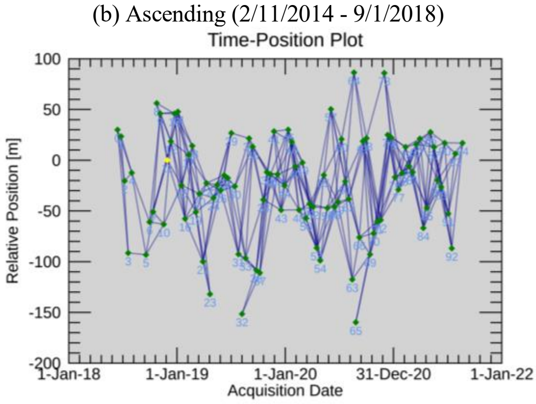

(c) Ascending (14/6/2018 – 21/8/2019)

Fig. 5 Connection graphs for SBAS-DInSAR analysis (yellow dot: super master data, green dot: SAR data)

5. RESULTS OF SBAS-DInSAR

(1) LOS displacement distribution

The SBAS-DInSAR analysis produced the time-transition of the spatial distribution of the displacements for each date of the SAR data acquisition. Therefore, a map of the displacement distribution was obtained almost every 10 days from 165 descending images and 152 ascending images during the last six or seven years. **Figs. 6** (a) and (b) show the last results, the final displacement distribution maps for the descending and ascending data, respectively. Green indicates no (0) or only small displacements of less than ±10 mm, and red and blue are negative (extension) and positive (compression) LOS displacements (see **Fig. 2**), respectively. Some areas on these maps do not show any results because of low coherence (less than the threshold) due to dense vegetation. The red line across the map represents the tunnel alignment (see **Fig. 3**).

It is found that the displacements are totally small, within a few cm, except the portion with red ("A") in the northeast section of the maps in both descending and ascending cases.

In order to see the details of the tunnel construction site, the displacement distribution is extracted for a band-shaped area along the tunnel alignment with a width of 500 m, as shown in **Fig. 7**. It is noted that the scale of the displacement in **Fig. 7** is different from the one in **Fig. 6**.

In both portions "M" around Mondeok IC (Inter Change) and "C" around Centum IC in **Fig. 7**, the descending LOS displacements are negative and the ascending LOS displacements are positive. On the other hand, there seem to be small displacements in portion "B" near the center of the tunnel alignment.

(2) Time-transition of displacements

The SBAS-DInSAR analysis can also produce the time-transition of the displacements at selected points.

Fig. 8 shows the time-transition of the LOS displacements in both descending and ascending cases at three points extracted from portion "A". A13 and A14 indicate the names of the points of interest in portion "A". It is found that both descending and ascending LOS displacements are negatively large, and that the descending displacements are larger than the ascending ones. No ascending results were obtained for A14

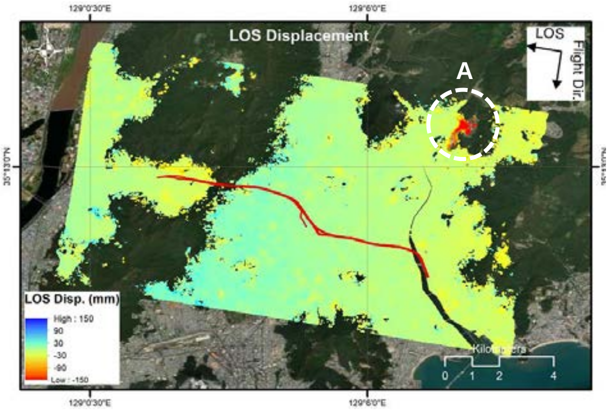

(a) Descending (2015-2021)

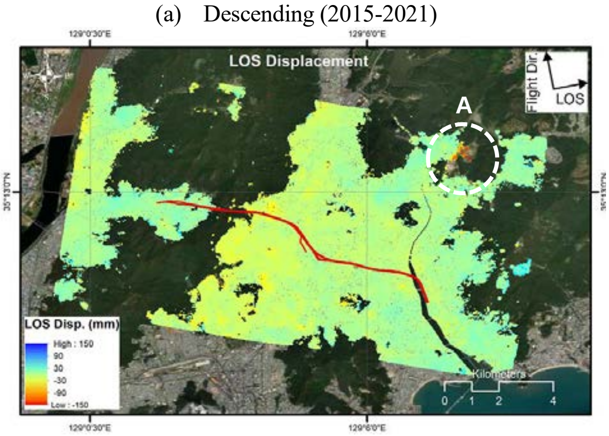

(b) Ascending (2014-2021 except a half year in 2018)

Fig. 6 LOS displacement distribution

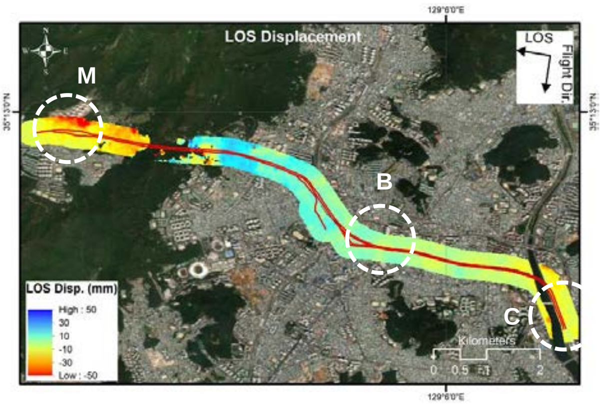

(a) Descending (2015-2021)

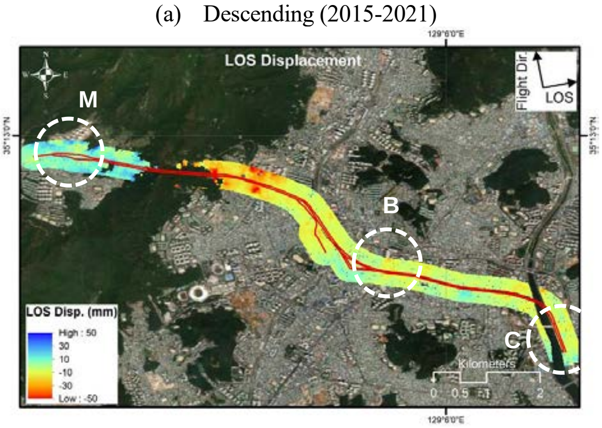

(b) Ascending (2014-2021 except a half year in 2018)

Fig. 7 LOS displacement distribution along tunnel alignment (red line) because of low coherence. By referring to **Fig. 9**[5)], the actual displacements can be estimated to be dominantly subsidence and to be slightly directed to the west. Since these points are located far from the tunnel, this behavior must have been caused by a different factor. Actually, portion "A" is located in an area of developed land, a mountainous area sloping to the west that was cut for the construction of a large park. This may be the cause of those displacements.

Figs. 10 to **12** present the time-transition of both descending and ascending LOS displacements at points extracted from portions "M", "B", and "C", respectively. In **Figs. 10** and **12**, the descending LOS displacements are negative, while the ascending ones are positive in portions "M" and "C" at the west and east portals of the tunnel. The absolute values of the descending displacements are almost the same as or slightly larger than those of the ascending ones. This means that the actual displacements can be estimated to face west.

In portion "C" (**Fig. 12**), near the central part of the tunnel, both descending and ascending LOS displacements are within 10 mm, which is the detection limit of displacements by the DInSAR method. It seems, therefore, that almost no or only quite small displacements have occurred in this portion.

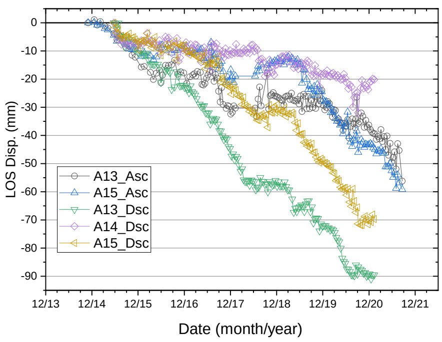

Fig. 8 Time-transition of LOS displacements in "A"

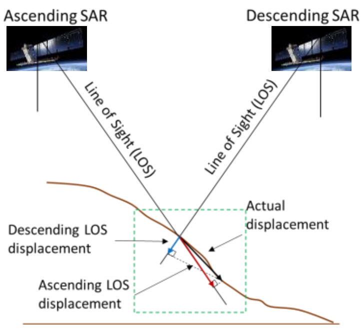

Fig. 9 Schematic diagram of geometrical relationship between actual and LOS displacements[5)]

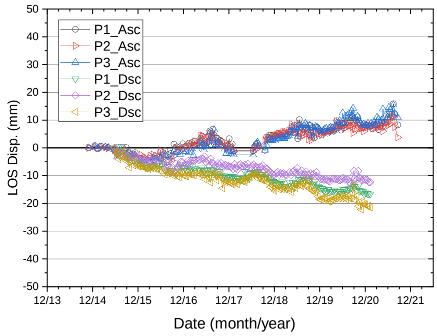

Fig. 10 Time-transition of LOS displacements in "M"

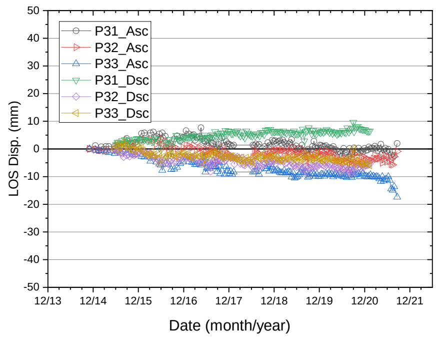

Fig. 11 Time-transition of LOS displacements in "B"

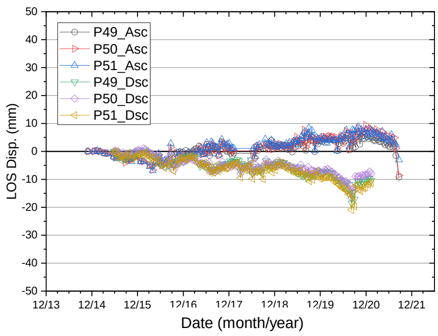

Fig. 12 Time-transition of LOS displacements in "C"

All displacements started to increase from the beginning of 2014 or 2015. As construction of the tunnel was begun in 2019 and only 10% of the project had been completed as of October 2021, those displacements could not have been caused by the tunnel construction.

6. CONCLUDING REMARKS

This paper has described the preliminary results of an investigation to clarify the applicability of DInSAR for monitoring the ground surface displacements above a tunnel construction site in Busan, Republic of Korea. The findings of this study are as follows:

- Large displacements were found at the northeast portion far from the tunnel construction site. Those displacements seem to have been caused by the land development around there.
- Displacements have increased in some areas since 2014 or 2015. Since construction of the tunnel was begun in 2019, those displacements had to have been caused by something other than the tunnel construction.
- At present, the tunnel construction is not known to have caused the occurrence of any displacements.

ACKNOWLEDGMENTS: This study was achieved as a project entitled “Development of Geotechnical Investigation Technique using Regional Image Data”, a national research and development project of the “Research Project of Advanced Technology for Construction and Operation of Underground Transportation Infrastructure”, and supported by the Korea Agency for Infrastructure Technology Advancement (KAIA), Research Project No. 21UUTI-B157786-02. The authors greatly appreciate the support of KAIA. They also extend their gratitude to Ms. H. Griswold for proofreading the manuscript.

REFERENCES

1) Ferretti, A. Satellite InSAR data: reservoir monitoring from space, EAGE Publication, The Netherlands, 2014.
2) Yastika, P. E., Shimizu, N. and Abidin, H. Z.: Monitoring of long-term land subsidence from 2003 to 2017 in coastal area of Semarang, Indonesia by SBAS DInSAR analyses using Envisat-ASAR, ALOS-PALSAR, and Sentinel-1A SAR data, *Advances in Space Research*, 63 , pp. 1719–1736, 2019.
3) Yastika, P. E., Shimizu, N., Pujianiki, N. N., Temaja, I G. R. M., Antara, I N. G. and Osawa, T.: Detection of silent subsidence over extensive area by SBAS DInSAR: a case study of Southern Bali, Indonesia, *Proc. CORECT-IJJSS 2019*, E3S Web Conference, Vol. 153, paper no. 02003, 2020.
4) Parwata, I N. S., Shimizu, N., Grujić, B., Zekan, S., Čeliković, R. and Vrkljan, I.: Monitoring the Subsidence Induced by Salt Mining in Tuzla, Bosnia and Herzegovina by SBAS-DInSAR Method, *Rock Mechanics and Rock Engineering*, 53(11), pp. 5155–5175, 2020.
5) Yastika, P. E., Shimizu, N. and Verbovšek, T.: A case study on landslide displacement monitoring by SBAS-DInSAR in the Vipava River Valley, Slovenia, *Proc. ISRM Specialized Conference YSRM2019*, pp. 406-411, 2019.
6) Nagasaki, K., Kameyama, M., Yoshimoto, M., Nakashima, S. and Shimizu, N.: Applicability of SBAS-DInSAR for Monitoring Displacements of a Local Steep Slope, *Proc. ISRM Specialized Conference RMEGV2021*, OS6-4, 2021.
7) Yamaguchi, M., Yastika, P. E., Shimizu, N., Milev, N. and Vrkljan, I.: Application of SBAS-DInSAR to monitoring landslides along the northern Black Sea coast in Bulgaria, *Proc. EUROCK-Torino 2021*, IOP Conf. Series: Earth and Environmental Science 833, paper no. 012151, 2021.
8) Parwata, I N. S., Nakashima, S., Shimizu, N. and Osawa, T.: Effect of digital elevation models on monitoring slope displacements in open-pit mine by Differential Interferometry Synthetic Aperture Radar, *Journal of Rock Mechanics and Geotechnical Engineering*, 12(5), pp. 1001-1013, 2020.
9) Yastika, P. E., Ibara, T., Shimizu, N., Iwata, N., Takahashi, H. and Araki, Y.: Application of DInSAR for Monitoring the Ground Deformation Due to Volcanic Activity: a Case Study of Sakurajima, *Proc. ISRM Regional Symposium: 10th Asian Rock Mechanics Symposium*, G2, 2018.
10) Parwata, I N. S., Nakashima, S. and Shimizu, N.: Monitoring Volcanic Activity of Mount Agung, Indonesia by SBAS-DInSAR Using Sentinel-1 Data from 2014 to 2020, *Proc. ISRM Specialized Conference: 5th International Workshop on Rock Mechanics and Engineering Geology in Volcanic Fields (RMEGV2021)*, OS4-1, 2021.
11) Yastika, P.E. and Shimizu, N.: Applications of DInSAR for ground surface deformation measurements-case studies of subsidence measurements and deformation detections due to an earthquake, *Proc. 37th West Japan Rock Engineering Symposium*, pp. 91-97, 2016.
12) Honda, K., Mushiake, N., Satoh, W., Satoh, H., Kobori, T., Sasaki, T., Yamaguchi, Y. and Shimizu, N.: New Application of Synthetic Aperture Radar (SAR) for Deformation Monitoring System, *Proc. the 2014 ISRM International Symposium: 8th Asian Rock Mechanics Symposium*, pp. 2512-2522, 2014.
13) Berardino P., Fornaro G., Lanari R. and Sansosti E.: A new algorithm for surface deformation monitoring based on small baseline differential SAR interferograms, *IEEE Trans. Geosci. Remote Sens*, 40, pp. 2375–2383, 2002.
14) https://www.hapskorea.com/mandeok-to-centum-city-highway-breaks-ground-this-month/ (3 Nov. 2021)
15) http://news.kmib.co.kr/article/view.asp?arcid=0013676221; http://www.busan.com/view/busan/view.php?code=2020020919194874840 (3 Nov. 2021)